[Article] doi: 10.3866/PKU.WHXB201205155 www.whxb.pku.edu.cn

新型螺吡喃衍生物: 离子传感和分子水平的信息处理

李颖若[1] 张洪涛[2] 齐传民[1,*] 郭雪峰[2,3,*]

([1]北京师范大学化学学院, 放射性药物教育部重点实验室, 北京 100875; [2]北京大学化学与分子工程学院, 北京分子科学国家实验室, 分子动态与稳态结构国家重点实验室, 北京 100871; [3]北京大学工学院先进材料与纳米技术系, 北京 100871)

摘要: 为实现金属离子检测和分子水平的信息处理, 合成了一类新型的含有功能配位基团的螺吡喃衍生物(**SP1**–**SP4**). 研究发现: 在没有UV光照的条件下, 金属离子可以促进螺吡喃(**SP2**和**SP4**)开环并形成稳定可逆的络合物(MC-M^{n+}). 紫外-可见吸收光谱研究表明, 在UV光照前加入不同的金属离子会引起**SP2**和**SP4**的光学性质的特征变化, 因此提供了一种简易的通过裸眼就能辨别金属离子的比色方法. 荧光光谱研究表明, 这类化合物能够高灵敏高选择性地检测锌离子. 此外, 基于吸收光谱和荧光光谱的变化, 这类螺吡喃衍生物可以用于构建组合的逻辑门, 执行分子水平的信息处理, 从而展现了其在化学或环境传感和未来的分子计算机领域的潜在应用前景.

关键词: 螺吡喃; 化学传感; 逻辑门; 紫外-可见吸收光谱; 荧光光谱

中图分类号: O641

New Spiropyran Derivatives: Ion Sensing and Information Processing at the Molecular Level

LI Ying-Ruo[1] ZHANG Hong-Tao[2] QI Chuan-Min[1,*] GUO Xue-Feng[2,3,*]

([1]*Key Laboratory of Radiopharmaceuticals, College of Chemistry, Beijing Normal University, Beijing 100875, P. R. China*; [2]*Beijing National Laboratory for Molecular Sciences, State Key Laboratory for Structural Chemistry of Unstable and Stable Species, College of Chemistry and Molecular Engineering, Peking University, Beijing 100871, P. R. China*; [3]*Department of Advanced Materials and Nanotechnology, College of Engineering, Peking University, Beijing 100871, P. R. China*)

Abstract: We have designed and synthesized a new class of spiropyran derivatives (**SP1**–**SP4**) with functional chelating groups, such as pyridine or quinoline moieties and a methoxy group (—OMe), for use in metal ion sensing and information processing at the molecular level. It is notable that metal ions can favor coordination with chelating groups and facilitate the photoisomerization of spiropyran molecules from the closed form to the open merocyanine form without UV irradiation, thus leading to significant changes in their chemical and physical properties. UV-Vis absorption studies indicated that **SP2** and **SP4** exhibited metal ion-dependent reversible binding affinities that result in different hypsochromic shifts for the MC-M^{n+} complexes. These changes in color can be recognized by eye, thus offering an easy colorimetric method for metal ion detection. Further emission studies distinguished them as promising candidates for Zn^{2+} detection with good sensitivity and selectivity. Moreover, on the basis of their absorption and fluorescence spectra, several combinational logic gates were constructed for information processing at the molecular level. These results demonstrate that spiropyran derivatives with desired functionalities show great potential not only for chemical or environmental sensors, but also for future molecular computing.

Received: March 31, 2012; Revised: May 14, 2012; Published on Web: May 15, 2012.

*Corresponding authors. GUO Xue-Feng, Email: guoxf@pku.edu.cn. QI Chuan-Min, Email: qichuanmin@bnu.edu.cn.

The project was supported by the National Key Basic Research Program of China (973) (2009CB623703, 2012CB921404), National Natural Science Foundation of China (20833001, 51121091, 2112016, 21071022), and Foundation for the Author of National Excellent Doctoral Dissertation of Higher Education, China (2007B21).

国家重点基础研究发展规划项目(973) (2009CB623703, 2012CB921404), 国家自然科学基金(20833001, 51121091, 2112016, 21071022)及全国高等学校优秀博士论文作者专项基金(2007B21)资助

Key Words: Spiropyran; Chemical sensor; Logic gate; UV-Vis absorption spectrum; Fluorescent spectrum

1 Introduction

Photochromic compounds have been extensively investigated in recent years for their high potential applications in optically rewritable storage,[1] optical switching,[2] chemical[3] and biological[4] sensings. In particular, considerable attention has been paid to spiropyran molecules, one of the most promising families of photochromic compounds, because of their unique optical and physical properties.[5−10] The stimulus-induced transformation of the ring-closed structure of spiropyrans (SPs) into their fully π-conjugated isomeric merocyanine forms (MCs) results not only in the variations of absorption spectra, but also in the profound alterations of other physical and chemical properties of the system, such as the dipole moments, nonlinear optic properties, emission spectra, and macroscopic properties (for example, conductance, rheological property, and surface wettability). By taking advantage of these remarkable characteristics of SPs, a number of spiropyran derivatives containing diverse functional groups have so far been designed and used as molecular sensors and molecular switches.[11−17]

Among the remarkable characteristics of SPs, one unique feature is that the photogenerated open merocyanine form processes the charge-separated zwitterionic state with a free negatively-charged oxygen atom, which can further interact with external stimuli through dipole−dipole interactions and coordination chemistry (Scheme 1). Recently, several groups have successfully utilized this for the purpose of optically detecting metal ions,[18−20] anions,[21] nucleobases,[22] amino acids,[23] and DNA,[24] etc. In this study, a new class of spirobenzopyrans **SP2** and **SP4** bearing electron-donating —OMe group and pyridine or quinoline moiety as binding sites were designed and synthesized (Scheme 1). We will explore the changes in their chemical and physical properties upon addition of different metal ions before and after UV irradiation and show the capability of selectively detecting metal ions with high sensitivity and constructing logic gates for information processing at the molecular level.[25−31]

2 Experimental

Functional spirobenzopyran derivatives **SP1**−**SP4** were synthesized as shown in Scheme 2. Compounds **2-1** and **2-2** were prepared by modification of the procedure reported by Raymo and Giordani[32] bearing —OH as a functional group for the following reaction step. The pyridine or quinoline moiety was then linked to compounds **2-1** and **2-2** using EDCI/DMAP (EDCI: 1-ethyl-3-(3-dimethylaminopropyl) carbodiimide, DMAP: 4-dimethylaminopyridine) esterification reaction to give **SP1**−**SP4** as yellow crystals in high yield (~90%).

2.1 1-(2-hydroxyethyl)-2,3,3-trimethylindoliumbromide (1)

Under nitrogen atmosphere, a mixture of 2,3,3-trimethyl-3*H*-indole (4.77 g, 30.0 mmol) and 2-bromoethanol (4.50 g, 36.0 mmol) in dry CH_3CN (30 mL) was heated under reflux for 12 h. Removal of CH_3CN and excess of 2-bromoethanol under the reduced pressure gave a dark purple residue. Repeated washing with anhydrous ether gave compound **1** (7.85 g, 92.1%) as a white solid. All the reagents used are AR grade.

^{1}H NMR (DMSO-d6, 400 MHz): 1.55 (s, 6H), 3.38 (s, 3H), 3.87 (t, 2H, J=6.8 Hz), 4.60 (t, 2H, J=6.8 Hz), 7.60−7.64 (m, 2H), 7.84−7.87 (m, 1H), 7.94−7.98 (m, 1H). Fourier transform mass spectroscopy (FTMS): m/z=204.1, $[M\text{-}Br]^+$.

2.2 2-(3′,3′-dimethyl-6-nitrospiro [chromene-2,2′-indolin]-1′-yl) ethanol (2-1)

Under nitrogen atmosphere, Compound **1** (1.14 g, 4.0 mmol) and 2-hydroxy-5-nitrob-enzaldehyde (0.80 g, 4.8 mmol) were dissolved in dry tetrahydrofuran (THF) (25 mL). The solution was heated to reflux then triethylamine (0.49 g, 4.8 mmol) in

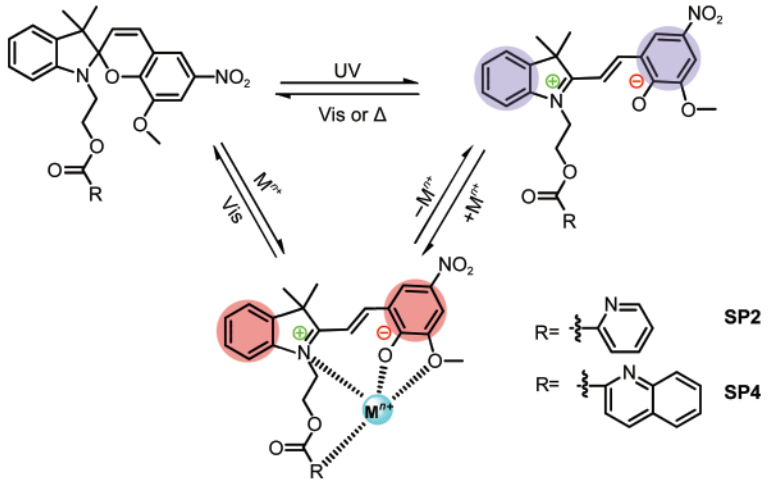

Scheme 1 Illustrations of the reversible structural transformations of SP2 and SP4 in responses to light, heat, and metal ions

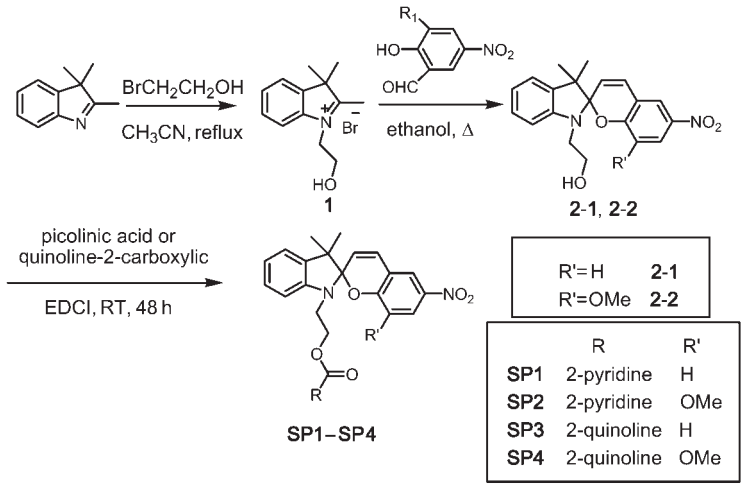

Scheme 2 Synthesis of spirobenzopyrans SP1–SP4

THF (5 mL) was added dropwise. The mixture was refluxed for 4 h. The solvent was removed by evaporation under reduced pressure. The crude residue was recrystallized from absolute ethanol giving compound **2-1** (1.30 g, 92.2%) as red purple crystals.

^{1}H NMR ($CDCl_3$, 400 MHz): 1.20 (s, 3H), 1.29 (s, 3H), 3.33–3.50 (m, 2H), 3.68–3.77 (m, 2H), 5.89 (d, 1H, *J*=13.6 Hz), 6.67 (d, 1H, *J*=10.4 Hz), 6.76 (d, 1H, *J*=12.4 Hz), 6.87–6.93 (m, 2H), 7.10 (d, 1H, *J*=9.0 Hz), 7.20 (t, 1H, *J*=10.0 Hz), 7.99–8.04 (m, 2H). FTMS: *m*/*z*=353.1, $[M+H]^+$.

2.3 2-(8-methoxy-3′,3′-dimethyl-6-nitrospiro [chromene-2,2′-indolin]-1′-yl) ethanol (2-2)

Compound **2-2** was prepared according to a procedure similar to compound **2-1**. After column chromatography on silica gel with ethyl acetate/petroleum (60–90 °C) (1:1, *V*/*V*) as eluent, compound **2-2** was obtained as dark blue crystals (3.82 g, 91.6%).

^{1}H NMR ($CDCl_3$, 400 MHz): 1.18 (s, 3H), 1.29 (s, 3H), 3.35–3.43 (m, 2H), 3.51–3.63 (m, 2H), 3.78 (s, 3H), 5.82 (d, 1H, *J*=14.0 Hz), 6.65 (d, 1H, *J*=10.4 Hz), 6.84–6.90 (m, 2H), 7.08 (d, 1H, *J*=10.0 Hz), 7.15–7.21 (m, 1H), 7.63 (d, 1H, *J*=3.6 Hz), 7.69 (d, 1H, *J*=3.6 Hz). FTMS: *m*/*z*=383.2, $[M+H]^+$.

2.4 2-(3′,3′-dimethyl-6-nitrospiro [chromene-2,2′-indolin]-1′-yl)ethylpicolinate (SP1)

Under nitrogen atmosphere, compound **2-1** (0.35 g, 1.0 mmol), picolinic acid (0.12 g, 1.0 mmol), EDCI (0.38 g, 2.0 mmol), DMAP (0.01 g, 0.1 mmol) were dissolved into dry dichloromethane (15 mL). The reaction mixture was stirred at room temperature overnight. Evaporation of the solvent gave a brown tar. The obtained brown tar was dissolved into ethyl acetate, washed with H_2O three times, and dried over anhydrous magnesium sulfate. Evaporation of the solvent gave a light brown residue. The crude residue was recrystallized from ethyl acetate/*n*-hexane giving **SP1** (0.82 g, 90.5%) as a light yellow crystals.

^{1}H NMR ($CDCl_3$, 400 MHz): 1.15 (s, 3H), 1.29 (s, 3H), 3.55–3.63 (m, 1H), 3.68–3.74 (m, 1H), 4.55–4.58 (m, 2H), 5.96 (d, 1H, *J*=10.4 Hz), 6.73 (d, 1H, *J*=8.4 Hz), 6.79 (d, 1H, *J*=8.0 Hz), 6.87–6.92 (m, 2H), 7.09 (d, 1H, *J*=6.4 Hz), 7.19–7.23 (m, 1H), 7.46–7.49 (m, 1H), 7.80-7.84 (m, 1H), 7.95–7.98 (m, 2H), 8.06 (d, 1H, *J*=7.2 Hz), 8.74 (d, 1H, *J*=4.8 Hz). ^{13}C NMR ($CDCl_3$, 100 MHz): 165.05, 159.32, 149.87, 147.72, 146.46, 141.06, 137.03, 135.75, 128.41, 127.92, 127.05, 125.92, 125.19, 122.76, 121.86, 121.83, 119.97, 118.45, 115.53, 106.78, 106.49, 63.30, 52.87, 42.21, 25.86, 19.85. FTMS: *m*/*z*=458.15, $[M+H]^+$.

2.5 2-(8-methoxy-3′,3′-dimethyl-6-nitrospiro [chromene-2,2′-indolin]-1′-yl) ethyl picolinate (SP2)

SP2 was prepared according to a procedure similar to **SP1**. Compound **2-2** was used instead of compound **2-1**. **SP2** was obtained as yellow crystals (0.64 g, 88.9%).

^{1}H NMR ($CDCl_3$, 400 MHz): 1.15 (s, 3H), 1.27 (s, 3H), 3.58–3.66 (m, 1H), 3.73 (s, 3H), 3.74–3.80 (m, 1H), 4.56 (t, 2H, *J*=6.6 Hz), 5.93 (d, 1H, *J*=10.4 Hz), 6.78 (d, 1H, *J*=7.6 Hz), 6.83–6.90 (m, 2H), 7.08 (d, 1H, *J*=6.4 Hz), 7.17–7.21 (m, 1H), 7.45–7.48 (m, 1H), 7.56 (d, 1H, *J*=2.8 Hz), 7.66 (d, 1H, *J*=2.4 Hz), 7.65–7.66 (m, 1H), 8.02 (d, 1H, *J*=7.6 Hz), 8.73 (d, 1H, *J*=5.6 Hz). ^{13}C NMR ($CDCl_3$, 100 MHz): 164.10, 149.84, 149.03, 147.73, 147.33, 146.42, 140.45, 136.99, 135.79, 128.36, 127.73, 126.99, 125.15, 121.88, 121.84, 119.68, 118.18, 115.30, 107.72, 106.70, 106.33, 63.27, 56.12, 52.84, 41.97, 25.98, 19.79. FTMS: *m*/*z*=488.19, $[M+H]^+$.

2.6 2-(3′,3′-dimethyl-6-nitrospiro [chromene-2,2′-indolin]-1′-yl) ethylisoquinol-ine-3-carboxylate (SP3)

SP3 was prepared according to a procedure similar to **SP1**. Quinoline-2-carboxylic was used instead of acid picolinic acid. **SP3** was obtained as light yellow crystals (0.69 g, 90.6%).

^{1}H NMR ($CDCl_3$, 400 MHz): 1.20 (s, 3H), 1.40 (s, 3H), 3.45–3.54 (m, 1H), 3.81–3.91 (m, 1H), 4.64–4.69 (m, 2H), 6.37 (d, 1H, *J*=14.4 Hz), 6.77 (d, 1H, *J*=10.4 Hz), 6.85–6.90 (m, 2H), 7.08 (d, 1H, *J*=10.0 Hz), 7.15–7.19 (m, 1H), 7.22 (d, 1H, *J*=11.6 Hz), 7.66–7.71 (m, 1H), 7.81–7.87 (m, 1H),

7.89−7.93 (m, 2H), 8.02 (d, 1H, *J*=4.0 Hz), 8.16 (d, 1H, *J*=11.6 Hz), 8.28−8.33 (m, 2H). ^{13}C NMR ($CDCl_3$, 100 MHz): 165.37, 159.41, 147.67, 147.57, 146.46, 141.00, 137.29, 135.78, 130.58, 130.44, 129.34, 128.79, 128.28, 127.93, 127.64, 125.87, 122.72, 122.27, 121.88, 120.95, 119.94, 118.54, 115.52, 106.75, 106.65, 63.54, 52.97, 42.30, 25.88, 19.88. FTMS: *m*/*z*=508.17, $[M+H]^+$.

2.7 2-(8-methoxy-3′,3′-dimethyl-6-nitrospiro [chromene-2,2′-indolin]-1′-yl) ethyl isoquinoline-3-carboxylate (SP4)

SP4 was prepared according to a procedure similar to **SP1**. Compound **2-2** was used instead of compound **2-1** and quinoline-2-carboxylic was used instead of acid picolinic acid. **SP4** was obtained as yellow crystals (0.72 g, 90.1%).

^{1}H NMR ($CDCl_3$, 400 MHz): 1.17 (s, 3H), 1.27 (s, 3H), 3.65−3.70 (m, 1H), 3.72 (s, 3H), 3.80−3.87 (m, 1H), 4.58−4.66 (m, 2H), 6.10 (d, 1H, *J*=10.4 Hz), 6.82 (d, 1H, *J*=7.6 Hz), 6.86 (d, 1H, *J*=10.4 Hz), 6.88 (t, 1H, *J*=7.4 Hz), 7.08 (d, 1H, *J*=6.4 Hz), 7.21 (t, 1H, *J*=7.6 Hz), 7.53 (d, 1H, *J*=2.4 Hz), 7.64 (d, 1H, *J*=2.4 Hz), 7.67 (t, 1H, *J*=8.0 Hz), 7.81 (t, 1H, *J*=7.6 Hz), 7.88 (d, 1H, *J*=9.2 Hz), 8.09 (d, 1H, *J*=8.8 Hz), 8.27 (d, 2H, *J*=8.4 Hz). ^{13}C NMR ($CDCl_3$, 100 MHz): 165.31, 149.12, 147.70, 147.54, 147.32, 146.42, 140.40, 137.22, 135.82, 130.56, 130.39, 129.28, 128.73, 128.26, 127.73, 127.60, 122.33, 121.86, 120.92, 119.64, 118.28, 115.28, 107.68, 106.67, 106.51, 63.50, 56.11, 52.95, 42.05, 25.97, 19.79. FTMS: *m*/*z*=538.17, $[M+H]^+$.

3 Results and discussion

3.1 Photochromic properties

Previous reports demonstrated that the introduction of an electron-withdrawing group (e.g., −NO_2, −CF_3) into the benzene ring enhances the stability of the open form of SPs[33,34] whereas an electron-donating group (e.g., −*t*-Bu, −OMe) produces a more stable photostationary closed form.[35,36] To gather the kinetic data of **SP1**−**SP4** to evaluate the effect of −OMe on the properties of spiropyrans, we monitored the evolutions of the absorption spectra and the time dependence of absorbance at λ_{max} (maximum absorption wavelength) of **SP1**−**SP4** in ethanol solution upon UV irradiation, visible irradiation and in the dark (Figs.S1−S4 (Supporting Information)). The kinetic of each process can be fit with a single exponential. Using the method from literature,[32,11] the rate constants and the percent conversions (χ_e) were calculated and summarized in Table 1. As expected, the rate constants for the conversions of **MC2** to **SP2** and **MC4** to **SP4** in the dark were determined to be ~(1.4±0.1)×10^{-2} s^{-1}, which is much larger than those for **MC1** to **SP1** (~(1.3±0.1)×10^{-3} s^{-1}) and **MC3** to **SP3** (~(1.7±0.1)×10^{-3} s^{-1}). This indicates that **MC2** and **MC4** can thermally isomerize back to the corresponding **SP2** and **SP4** faster than the cases of **SP1** and **SP3**. Visible irradiation can accelerate the conversion from MC to SP. Consistently, the rate constants for **MC2** to **SP2** (~(1.1±0.1)×10^{-1} s^{-1}) and **MC4** to **SP4** (~(8.9±0.1)×10^{-2} s^{-1}) under visible irradiation are still larger than those for **MC1** to **SP1** (~(7.2±0.1)×10^{-3} s^{-1}) and **MC3** to **SP3** (~(7.1±0.1)×10^{-3} s^{-1}), separately. On the basis of kinetic data listed in Table 1, the calculated conversions (χ_e) of **SP2** and **SP4** are 6.7% and 8.7%, respectively, which are much smaller than the cases for **SP1** and **SP3** (56.4% and 50.3%, respectively), indicating that the introduction of −OMe apparently shifts the SP/MC equilibrium to favor the closed form of spiropyrans and thus decrease the stability of the open form most likely due to the increase of the electron density of the phenoxide ion unit affected by the electron-donating −OMe group.[19]

Table 1 Calculated rate constants and conversions of SP1−SP4 at 293 K

Compound	K_{UV}/s^{-1}	K_{dark}/s^{-1}	$K_{visible}$/s^{-1}	χ_e/%
SP1	(1.1±0.1)×10^{-2}	(1.3±0.1)×10^{-3}	(7.2±0.1)×10^{-3}	56.4
SP2	(9.2±0.1)×10^{-3}	(1.4±0.1)×10^{-2}	(1.1±0.1)×10^{-1}	6.7
SP3	(8.9±0.1)×10^{-3}	(1.7±0.1)×10^{-3}	(7.1±0.1)×10^{-3}	50.3
SP4	(9.8±0.1)×10^{-3}	(1.4±0.1)×10^{-2}	(8.9±0.1)×10^{-2}	8.7

K_{UV}: the rate constant for the conversions of SP to MC upon UV irradiation; K_{dark}: the rate constant for the conversions of MC to SP in the dark; $K_{visible}$: the rate constant for the conversions of MC to SP under visible irradiation; χ_e: the calculated conversion

3.2 Sensing properties

Fig.1 and Fig.S5 (Supporting Information) show the absorption spectra of **SP1**−**SP4** (5.0×10^{-5} mol·L^{-1}) in ethanol in the absence and the presence of 1 equivalent (equiv.) of different

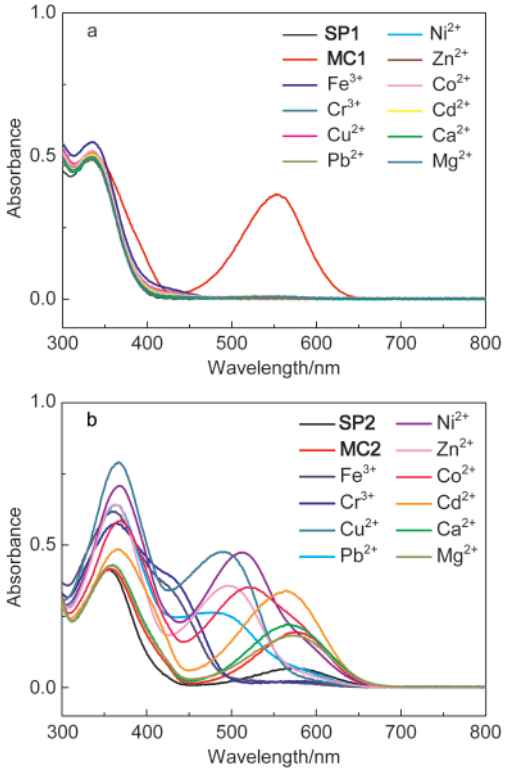

Fig.1 Absorption spectra of SP1 (a) and SP2 (b) after addition of 1 equivalent of different metal ions in the dark

concentrations of **SP1** and **SP2**: 5.0×10^{-5} mol·L^{-1}, solvent: ethanol, temperature: 293 K

metal ions before and after UV irradiation. Interestingly, we found that the spectra for the solutions of **SP2** and **SP4** after addition of metal ions were significantly changed depending on the kind of metal ions (Figs.1b and S5a) whereas no obvious spectral changes were observed for control compounds **SP1** and **SP3** (Figs.1a and S5b) before UV irradiation. In contrast, after further UV irradiation, **SP1**/**SP3** showed the obvious absorption changes in the presences of different metal ions (Fig. S5(c, d)) whereas **SP2**/**SP4** showed the negligible spectral changes (data not shown). Tables 2 and S1 give a summary of the maximum absorption wavelength (λ_{max}) of **SP1**–**SP4** in the absence and the presence of different metal ions after UV irradiation and the corresponding changes in maximum absorption wavelengths ($\Delta\lambda_{max}$).

On the basis of data in Tables 2 and S1, we found that the absorbance maxima of **SP1** and **SP3** in the presence of metal ions after UV irradiation showed the hyperchromatic shifts to different extents depending on different metal ions (Summaries of some important parameters for different metal ions can be found in Table S2 and Fig.S6). After separate additions of Fe^{3+}, Cr^{3+}, Cu^{2+}, and Pb^{2+}, the shoulder peaks at ~400–450 nm with the large hypsochromic shifts of >100 nm appeared due to the formation of MC-M^{n+} complexes (Scheme 1), showing that the interactions between metal ions and MC are very strong. In the cases of Zn^{2+}, Ni^{2+}, Co^{2+}, and Cd^{2+}, only slight hypsochromic shifts of 9–14 nm were observed after addition of them, reflecting that the interactions between metal ions and MC are moderate. However, the maximum absorption wavelength (λ_{max}) of MC did not change at all upon addition of Ca^{2+} and Mg^{2+}, showing that the interactions between Ca^{2+}/Mg^{2+} and MC are quite weak. Fig.S7(a, b) shows the corresponding photographs of **SP1** upon addition of 1 equiv. of metal ions before and after UV irradiation, respectively, from which the observed color changes are consistent with UV-Vis absorption studies discussed above. Further irradiation of the UV-irradiated solutions of **SP1** and **SP3** with visible light can turn all of them back to the original. In conjunction with UV-Vis studies before UV irradiation in Figs.1a and S5b, these results demonstrate that only the addition of metal ions can not lead to the conversion of **SP1** and **SP3** from the close form to the open form and that upon UV irradiation, metal ions can reversibly interact with the photoreleased negatively-charged phenolate oxygen with the different strengths and form MC-M^{n+} complexes.

Table 2 Summaries of the maximum absorption wavelengths (λ_{max}) of SP1 and SP2 in ethanol solution in the absence and presence of different metal ions and the corresponding changes in λ_{max} ($\Delta\lambda_{max}$) after UV irradiation

Metal ion	SP1		SP2	
	λ_{max}/nm	$\Delta\lambda_{max}$/nm	λ_{max}/nm	$\Delta\lambda_{max}$/nm
none	552		576	
Fe^{3+}	~420	>100	~420	>100
Cr^{3+}	~420	>100	~420	>100
Pb^{2+}	~420	>100	480	96
Cu^{2+}	~420	>100	490	86
Cd^{2+}	538	14	566	10
Co^{2+}	540	12	516	60
Zn^{2+}	543	9	497	79
Ni^{2+}	540	12	512	64
Ca^{2+}	552	0	568	8
Mg^{2+}	552	0	573	3

Remarkably, we found that only addition of metal ions led to the ring-opening isomerization of **SP2** and **SP4** with distinct color changes as shown in Figs.1b and S5a. For example, addition of Fe^{3+} and Cr^{3+} produced an immediate color changes from colorless to brilliant yellow. Correspondingly, a shoulder at about 420 nm, a significant hypsochromic shift in comparison with the open form,[37] was observed, which should be ascribed to MC-M^{n+} complexes as demonstrated above. Irradiating the colored solution with visible light did not liberate metal ions with regeneration of the original absorbance, showing the strong interactions between metal ions and MC. It is well known that metal ions with high charge density (Z^2/r, where Z is the ion charge and r is the ionic radius) tend to form firm combinations with ligands.[19,38–40] Among metal ions studied here, both Cr^{3+} and Fe^{3+} possessing more charges and relatively smaller ionic radii afford a higher charge density, consistent with the experimental observation. In comparison with **SP1** and **SP3**, we hypothesize that the metal-generated ring opening of SP should be ascribed to the synergistic effect of the strong affinity between metal ions and SP and the presence of the －OMe group that favors the formation of stable chelate complexes (MC-M^{n+}). When transition metals, such as Cu^{2+}, Zn^{2+}, Ni^{2+}, Co^{2+} and an IVA group metal ion Pb^{2+} were used, the hypsochromic shifts in absorbance maxima in the range of 60–96 nm were detected. From Fig.S6, we can see that these metal ions have smaller but approximate charge density, thus resulting in the moderate binding between metal ions and MC that affords the reversible photochromism upon exposure to visible light. These also led to different hypsochromic shifts of λ_{max} of the resulted MC-M^{n+} complexes with the different colors that can be differentiated by a naked eye (Fig.S7(c, d)). For example, an orange color was observed for the Cu^{2+} and Pb^{2+} complexes with λ_{max} of 490 and 480 nm, respectively, while a pink color was observed for Ni^{2+} and Co^{2+} complexes with λ_{max} of 512 and 516 nm, respectively. The absorbance maxima of Zn^{2+} complex (497 nm) was situated between them with a pink-orange color. In contrast, in the presence of Ca^{2+}, Mg^{2+}, and Cd^{2+}, the absorption spectra change only slightly whenever spiropyran molecules were closed or open, reflecting that the interactions between metal ions and molecules are weak. For the alkaline-earth metal ions Mg^{2+} and Ca^{2+}, the missing of *d* electrons may decrease the coordination ability of metal ions with SP. Cd^{2+} is another metal ion of group IIB similar to Zn^{2+}, but the hypsochromic shift in absorbance maxima of Cd^{2+} is smaller than that observed with Zn^{2+} probably because of the larger

size of Cd^{2+} (ionic radius=97 pm) relative to Zn^{2+} (ionic radius= 74 pm). The findings demonstrate that the interactions of metal ions with **SP2** and **SP4** are highly metal ion-dependent, thus potentially providing a useful colorimetric approach for detecting different metal ions with high sensitivity.

To further detect the capability of ion sensing, we investigated the emission properties of **SP1–SP4**. When excited at the maximum absorption wavelength of **SP1–SP4**/**MC1–MC4**, it was found that the closed forms **SP1–SP4** had no emission while the zwitterionic opened forms **MC1–MC4** fluoresced with the maximum absorption wavelengths of ca 626, 650, 636, and 660 nm (Fig.2a), respectively, consistent with the previous report.[41] Importantly, addition of 1 equiv. of Zn^{2+} to the **SP2** solution led to a dramatic increase in emission intensity at 600 nm excited at λ=493 nm. Similar results were obtained with **SP4** (Fig.S8). The fluorescence increase is majorly due to the coordination of Zn^{2+} with —OMe and fluorophores (pyridine or quinoline moiety) together with phenolate oxygen. The coordination can decrease the electron densities of the —OMe and the phenolate oxygen and thus increase the π-conjugation degree of the complex. On the other hand, the coordination of the ligands with the diamagnetic Zn^{2+} containing a closed-shell d^{10} electronic configuration would shut down the photoinduced electron-transfer pathway of the excited free ligand upon Zn^{2+} coordination[42–44] and thus turn on the fluorescence. Another possibility is that the coordination would inhibit the photoinduced tautomerization of the phenolate moiety which leads to nonradiative deexcitation and thus improve the fluorescence by reducing the probability of radiationless relaxation.[45,46]

Addition of metal ions such as Pb^{2+}, Mg^{2+}, Cd^{2+} to the solution of **SP2** or **SP4** also resulted in the fluorescence enhancement. However, the magnitude of the fluorescent enhancement of **SP2** or **SP4** in the presence of them is smaller than that observed with Zn^{2+}, which could be attributed to the different binding affinities of pyridine and quinoline with them. Ca^{2+} cannot turn on the fluorescence because of the larger ionic size (ionic radius=99 pm) and relative lower ionic electronegativity (1.01). Other metal ions studied, such as Fe^{3+}, Cr^{3+}, Cu^{2+}, Co^{2+}, and Ni^{2+}, were unable to turn on the fluorescent signal of **SP2** or **SP4**, which may be attributed to the proximity of the paramagnetic metal ions to the unpaired electrons of the ligands which lead to spin-orbit coupling and intersystem crossing.[47] To further explore the selectivity of Zn^{2+}, competition experiments were also conducted in which solutions of **SP2** or **SP4** was first added with 1 equiv. of other metal ions separately and Zn^{2+} was then added to the mixture. As shown in Figs.2d and S8b, the fluorescence of **SP2** or **SP4** after addition of Zn^{2+} dramatically increased, demonstrating the excellent selectivity of Zn^{2+} detection. It should be noted that the fluorescence increase was relatively small when Zn^{2+} was added to the solution of **SP2** in the presence of 1 equiv. of Fe^{3+}, Cr^{3+}, and Cu^{2+}. This may be ascribed to the stronger coordination of the metal ions with the ligands as is already clear from the absorption spectra analysis. Finally, the bingding mode of the complex was studied by Job′s plot analysis. Fig.3a shows the typical UV-Vis spectroscopic responses of a **SP2** ethanolic solution containing Zn^{2+} with the increasing concentrations. The absorbance at 576 nm decreased and the absorbance at 350 and 497 nm increased with the concentration increase. The stoichiometry of the zinc complex has been investigated *via* Job′s method (Figs.3b and S9) and it has been found to be 1:1. Note that the detection of metal ions should be also performed in water or other polar solvents since **SP1–SP4** could be readily soluble in these solvents with aid of ethanol.

3.3 Combinational logic circuits

As mentioned above, **SP2** and **SP4** response to the stimuli of metal ions and visible light, accompanying significant changes in physical and chemical properties. By taking use of these features, logic gates and combinational logic circuits can be constructed. It is well known that, the three basic types of logic gates are NOT, AND, and OR gates. The NOT gate is often called inverter which can converts the input signal (I) of 1 into the output signal (O) of 0 and *vice versa*. In the instant of AND gate, output O is 1 only when both inputs I_1 and I_2 are 1. The OR gate also combines the two inputs I_1 and I_2 into the output O, when I_1 and/or I_2 is 1, O is 1. Combinational logic circuits are assembled connecting NOT, AND, and OR gates. The inhibit (INH) gates are basic AND gates with one of the inputs inverted through a NOT function. Several examples of INH gate based on molecules have been reported in recent years.[48–50] Fig.4 illustrates that **SP2** (or **SP4**) can work as an INH logic gate upon the stimulation of metal ions and visible light. The two inputs signals are $I_1(Zn^{2+})$ and I_2(Vis) and the output is O, the absorbance maxima of the complex (A_{497}) or the fluorescence emission intensity at 600 nm (F_{600}). According to the results of the spectral study, the increase in the absorbance maxima of the complex or the emission intensity at 600 nm is observed only in the presence of Zn^{2+} and the absence of visible light. That is to say, only when I_1=1 and I_2=0, the output signal O=1. O is always 0 in other cases.

In particular, using the new photochromic compounds **SP2** and **SP4**, we can develop more complicated combinational logic circuits to convert three inputs into two outputs. In the case of the combinational logic circuit shown in Fig.5, the three inputs signals are $I_1(Zn^{2+})$, $I_2(Ni^{2+})$, and I_3(Vis) and the two outputs are $O_1(A_{497})$ and $O_2(F_{600})$. Binary digits can be encoded on each signal applying positive logic conventions (low=0, high= 1). Consequently, **SP2** (or **SP4**) can read a string of three binary inputs and write two specific optical outputs. The corresponding truth table and equivalent logic circuit are demonstrated in Fig.5. One portion of this logic circuit converts the three inputs I_1, I_2, and I_3 into the output O_1 through OR, NOT, and AND operations. The other fragment transduces the inputs of I_1 and I_3 into the output O_2 through NOT and AND operations. The optical output O_1 is high (O_1=1) when only the input I_1 is applied (I_1=1, I_2=0, I_3=0) or when only the input I_2 is ap-

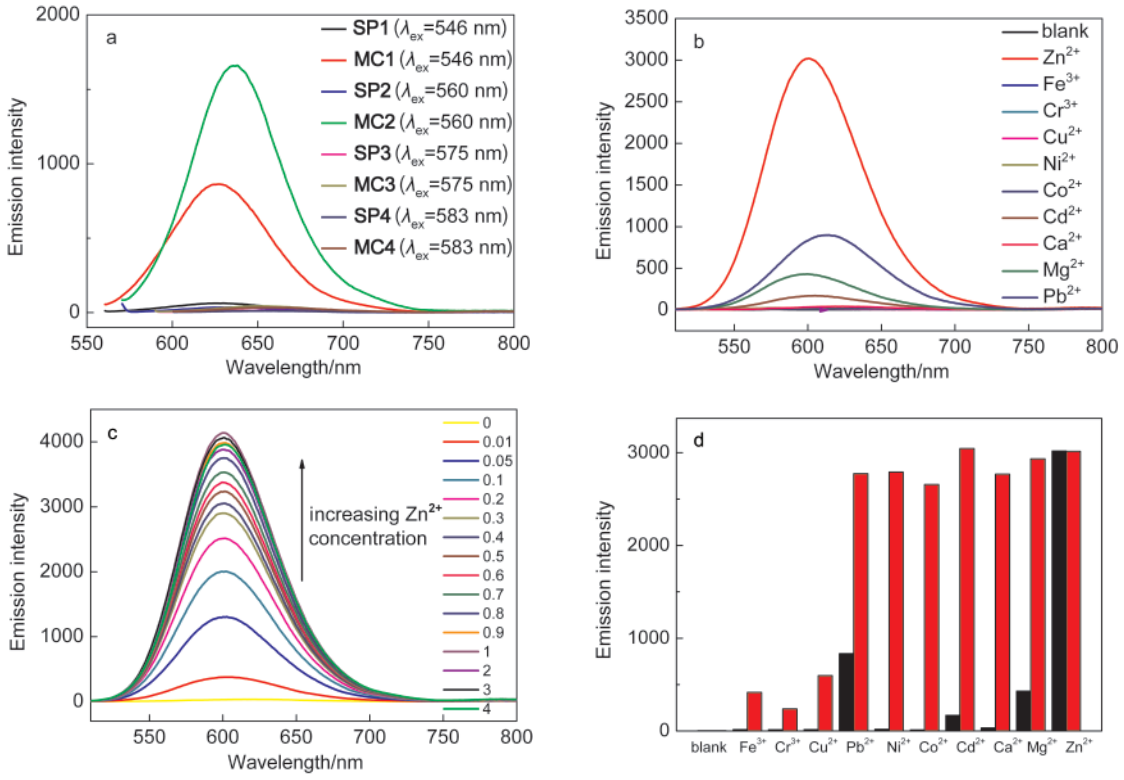

Fig.2 (a) Fluorescence emission spectra of SP1–SP4/MC1–MC4; (b) fluorescence emission spectra (λ_{ex}=493 nm) of SP2 (5.0×10^{-5} mol·L^{-1}, ethanol, 293 K) upon addition of 1 equiv. of metal ions (Zn^{2+}, Fe^{3+}, Cr^{3+}, Cu^{2+}, Ni^{2+}, Co^{2+}, Cd^{2+}, Ca^{2+}, Mg^{2+}, and Pb^{2+}); (c) changes in fluorescence emission spectra (λ_{ex}=493 nm) of SP2 (5.0×10^{-5} mol·L^{-1}, ethanol, 293 K) upon addition of different concentrations of Zn^{2+}; (d) detection selectivity of SP2 (5.0×10^{-5} mol·L^{-1}, ethanol, 293 K) in the presence of various metal ions (λ_{ex}=493 nm): (black bars) fluorescence emission intensity at 600 nm in the presence of 1 equiv. of Fe^{3+}, Cr^{3+}, Cu^{2+}, Pb^{2+}, Ni^{2+}, Co^{2+}, Cd^{2+}, Ca^{2+}, Mg^{2+}, and Zn^{2+}; (red bars) fluorescence emission intensity at 600 nm after further addition of 1 equiv. of Zn^{2+}

plied (I_1=0, I_2=1, I_3=0) or when only the input I_3 is not applied (I_1=1, I_2=1, I_3=0) (Fig.S10a). The optical output O_2 is high (O_2=1) when only the input I_1 is applied (I_1=1, I_2=0, I_3=0) or when only the input I_3 is not applied (I_1=1, I_2=1, I_3=0). The combinational logic circuit shows that all three inputs determine the output O_1, while only I_1 and I_3 control the value of O_2.

As mentioned above, in the combinational logic circuit illustrated in Fig.5, one of the output O_2 was not affected by the input I_2, while in the instance of the logic circuit shown in Fig.6, both the outputs O_1 and O_2 are dependent on the three inputs I_1, I_2, and I_3. The combinational logic circuit also consists of three inputs, two of which are chemical inputs $I_1(Zn^{2+})$ and $I_2(Cu^{2+})$ and the other is optical input I_3(Vis), the two outputs are O_1 (A_{497}) and $O_2(F_{600})$. When positive conventions are applied to all signals, the two independent optical outputs (O_1 and O_2) can be modulated by stimulating the molecular switch (**SP2** or **SP4**) with the three terminal inputs (I_1, I_2, and I_3). According to the fluorescence spectral study, addition of Cu^{2+} to the solution of **SP2** (or **SP4**) containing 1 equiv. Zn^{2+} can cause the fluorescence quenching. Then, the output O_2 is closely related to the

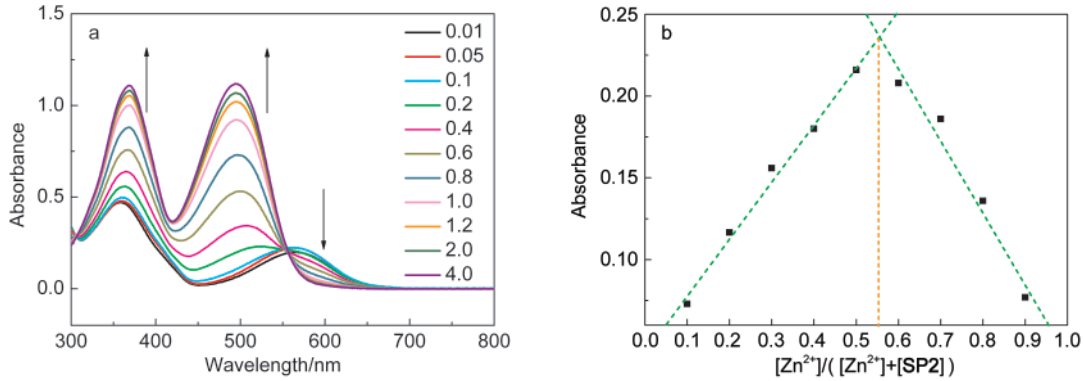

Fig.3 (a) UV-Vis spectroscopic response of SP2 ethanolsolution containing Zn^{2+} with the increasing concentrations; (b) Job′s plot of SP2 with Zn^{2+} in ethanol solution

(b) Total concentration of [**SP2**]+[Zn^{2+}] was kept constant. The absorbance at 497 nm was used.

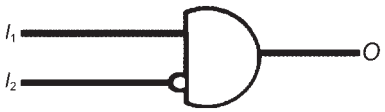

I_1(Zn^{2+})	I_2(Vis)	O(A_{497} or F_{600})
0	0	0
1	0	1
0	1	0
1	1	0

Fig.4 Truth table (bottom) and INH logic gate with two inputs and one output (up)

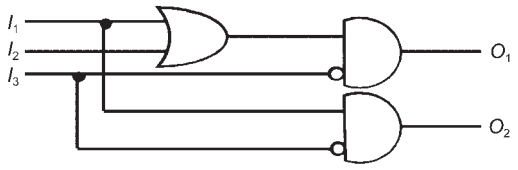

I_1(Zn^{2+})	I_2(Ni^{2+})	I_3(Vis)	O_1(A_{497})	O_2(F_{600})
0	0	0	0	0
1	0	0	1	1
0	1	0	1	0
0	0	1	0	0
1	1	0	1	1
0	1	1	0	0
1	0	1	0	0
1	1	1	0	0

Fig.5 Truth table (bottom) and corresponding combinational logic circuits with three inputs and two outputs (up)

The three inputs are I_1(Zn^{2+}), I_2(Ni^{2+}), and I_3(Vis) and the two outputs are O_1(A_{497}) and O_2(F_{600}).

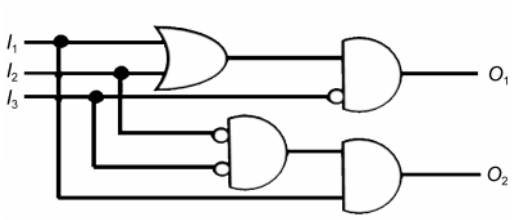

I_1(Zn^{2+})	I_2(Cu^{2+})	I_3(Vis)	O_1(A_{497})	O_2(F_{600})
0	0	0	0	0
1	0	0	1	1
0	1	0	1	0
0	0	1	0	0
1	1	0	1	0
0	1	1	0	0
1	0	1	0	0
1	1	1	0	0

Fig.6 Truth table (bottom) and the equivalent logic circuits based on SP2 or SP4 (up)

The three inputs are I_1(Zn^{2+}), I_2(Cu^{2+}) and I_3(Vis) and the two outputs are O_1(A_{497}) and O_2(F_{600}).

presence and the absence of Cu^{2+}. Therefore, the output O_2 is high when only the input I_1 is applied (I_1=1, I_2=0, I_3=0), and both I_2 and I_3 are inhibiting factors to O_2. As for the other output O_1, the absorbance maximum of the complex is high upon addition of Zn^{2+} and 1 equiv. Cu^{2+} in the absence of visible light (Fig.S10b). Accordingly, O_1 is high (O_1=1) when only I_1 is applied (I_1=1, I_2=0, I_3=0) or when only I_2 is applied (I_1=0, I_2=1, I_3=0) or when only I_3 is not applied (I_1=1, I_2=1, I_3=0). It can be seen from the truth table and the corresponding logic circuit, the inputs I_1, I_2 and I_3 are transmitted into output O_1 through OR, NOT, and AND operations while the output O_2 through NOT and AND operations.

4 Conclusions

In this work, we demonstrate the use of spiropyran derivatives incorporating the chelating sites, such as the pyridine or quinoline moiety and methoxy group, into their backbones for creating chemical sensors with high sensitivity and selectivity and combinational logic gates for information processing at the molecular level. The coordination of metal ions with －OMe and pyridine or quinoline moiety facilitates the photoisomerization of spiropyran molecules from the closed form to the open merocyanine form with and even without UV irradiation, accompanying with the significant changes in their chemical and physical properties. UV-Vis absorption studies demonstrated that **SP2** and **SP4** showed the metal ion-dependent reversible binding affinities that led to the different hypsochromic shifts of the absorption of MC-M^{n+} complexes with different colors. The color changes can be recognized by a naked eye, thus offering an easy colorimetric method for metal ion detection. On the other hand, the fluorescence measurements proved the unique property of **SP2** and **SP4** for selectively detecting Zn^{2+} with high sensitivity. In combination with both UV-Vis absorption and fluorescence changes under external stimuli, molecular systems based on **SP2** and **SP4** have been configured to mimic the functions of several integrated logic gates, suggesting attractive prospects in detecting, elaborating, and transmitting signals at the molecular level or even future molecular computing.

References

(1) Irie, M. *Chem. Rev.* **2000,** *100*, 1685. doi: 10.1021/cr980069d

(2) Irie, M.; Fukaminato, T.; Sasaki, T.; Tamai, N.; Kawai, T. *Nature* **2002,** *420*, 759. doi: 10.1038/420759a

(3) de Silva, A. P.; Gunaratne, H. Q. N.; Gunnlaugsson, T.; Huxley, A. J. M.; McCoy, C. P.; Rademacher, J. T.; Rice, T. E. *Chem. Rev.* **1997,** *97*, 1515. doi: 10.1021/cr960386p

(4) Kocer, A.; Walko, M.; Meijberg, W.; Feringa, B. L. *Science* **2005,** *309*, 755. doi: 10.1126/science.1114760

(5) Berkovic, G.; Krongauz, V.; Weiss, V. *Chem. Rev.* **2000,** *100*, 1741. doi: 10.1021/cr9800715

(6) Guo, X.; Zhang, D.; Zhu, D. *Adv. Mater.* **2004,** *16*, 125. doi: 10.1002/adma.200306102

(7) Kawata, S.; Kawata, Y. *Chem. Rev.* **2000,** *100*, 1777. doi: 10.1021/cr980073p

(8) Delaire, J. A.; Nakatani, K. *Chem. Rev.* **2000,** *100*, 1817. doi: 10.1021/cr980078m

(9) Tamai, N.; Miyasaka, H. *Chem. Rev.* **2000,** *100*, 1875. doi: 10.1021/cr9800816

(10) Guo, X.; Zhang, D.; Yu, G.; Wan, M.; Li, J.; Liu, Y.; Zhu, D. *Adv. Mater.* **2004,** *16*, 636. doi: 10.1002/adma.200305792

(11) Shen, Q.; Wang, L.; Liu, S.; Cao, Y.; Gan, L.; Guo, X.; Steigerwald, M. L.; Shuai, Z.; Liu, Z.; Nuckolls, C. *Adv. Mater.* **2010,** *22*, 3282. doi: 10.1002/adma.201000471

(12) Guo, X.; Huang, L.; O′Brien, S.; Kim, P.; Nuckolls, C. *J. Am. Chem. Soc.* **2005,** *127*, 15045. doi: 10.1021/ja054335y

(13) Lee, H. Y.; Diehn, K. K.; Sun, K.; Chen, T.; Raghavan, S. R. *J. Am. Chem. Soc.* **2011,** *133*, 8461. doi: 10.1021/ja202412z

(14) Vlassiouk, I.; Park, C. D.; Vail, S. A.; Gust, D.; Smirnov, S. *Nano Lett.* **2006,** *6*, 1013. doi: 10.1021/nl060313d

(15) Guo, X.; Zhang, D.; Tao, H.; Zhu, D. *Org. Lett.* **2004,** *6*, 2491. doi: 10.1021/ol0494111

(16) Zhang, H.; Guo, X.; Hui, J.; Hu, S.; Xu, W.; Zhu, D. *Nano Lett.* **2011,** *11*, 4939. doi: 10.1021/nl2028798

(17) Jiang, G.; Song, Y.; Guo, X.; Zhang, D.; Zhu, D. *Adv. Mater.* **2008,** *20*, 2888. doi: 10.1002/adma.200800666

(18) Shao, N.; Zhang, Y.; Cheung, S.; Yang, R.; Chan, W.; Mo, T.; Li, K.; Liu, F. *Anal. Chem.* **2005,** *77*, 7294. doi: 10.1021/ac051010r

(19) Sakamoto, H.; Takagaki, H.; Nakamura, M.; Kimura, K. *Anal. Chem.* **2005,** *77*, 1999. doi: 10.1021/ac048642i

(20) Inouye, M.; Akamatsu, K.; Nakazumi, H. *J. Am. Chem. Soc.* **1997,** *119*, 9160. doi: 10.1021/ja9707668

(21) Shiraishi, Y.; Adachi, K.; Itoh, M.; Hirai, T. *Org. Lett.* **2009,** *11*, 3482. doi: 10.1021/ol901399a

(22) Takase, M.; Inouye, M. *Chem. Commun.* **2001,** 2432.

(23) Shao, N.; Jin, J. Y.; Cheung, S. M.; Yang, R. H.; Chan, W. H.; Mo, T. *Angew. Chem. Int. Edit.* **2006,** *45*, 4944. doi: 10.1002/anie.200600112

(24) Andersson, J.; Li, S.; Lincoln, P.; Andréasson, J. *J. Am. Chem. Soc.* **2008,** *130*, 11836. doi: 10.1021/ja801968f

(25) de Silva, A. P.; Gunaratne, H. Q. N.; McCoy, C. P. *Nature* **1993,** *364*, 42. doi: 10.1038/364042a0

(26) de Silva, A. P.; Gunaratne, H. Q. N.; McCoy, C. P. *J. Am. Chem. Soc.* **1997,** *119*, 7891. doi: 10.1021/ja9712229

(27) de Silva, A. P.; McClenaghan, N. D. *J. Am. Chem. Soc.* **2000,** *122*, 3965. doi: 10.1021/ja994080m

(28) Guo, X.; Zhang, D.; Zhou, Y.; Zhu, D. *J. Org. Chem.* **2003,** *68*, 5681. doi: 10.1021/jo034243w

(29) Raymo, F. M. *Adv. Mater.* **2002,** *14*, 401. doi: 10.1002/1521-4095(20020318)14:6<401::AID-ADMA401>3.0.CO;2-F

(30) Guo, X.; Zhang, D.; Zhang, G.; Zhu, D. *J. Phys. Chem. B.* **2004,** *108*, 11942. doi: 10.1021/jp047706q

(31) Guo, X.; Zhang, D.; Wang, T.; Zhu, D. *Chem. Commun.* **2003,** 914.

(32) Raymo, F. M.; Giordani, S. *J. Am. Chem. Soc.* **2001,** *123*, 4651. doi: 10.1021/ja005699n

(33) Hirano, M.; Osakada, K.; Nohira, H.; Miyashita, A. *J. Org. Chem.* **2001,** *67*, 533.

(34) Guo, X.; Zhou, Y.; Zhang, D.; Yin, B.; Liu, Z.; Liu, C.; Lu, Z.; Huang, Y.; Zhu, D. *J. Org. Chem.* **2004,** *69*, 8924. doi: 10.1021/jo0487799

(35) Shao, N.; Jin, J.; Wang, H.; Zheng, J.; Yang, R.; Chan, W.; Abliz, Z. *J. Am. Chem. Soc.* **2009,** *132*, 725.

(36) Natali, M.; Soldi, L.; Giordani, S. *Tetrahedron* **2010,** *66*, 7612. doi: 10.1016/j.tet.2010.07.035

(37) Fries, K. H.; Driskell, J. D.; Samanta, S.; Locklin, J. *Anal. Chem.* **2010,** *82*, 3306. doi: 10.1021/ac1001004

(38) Paramonov, S. V.; Lokshin, V.; Fedorova, O. A. *J. Photochem. Photobiol. C: Photochem. Rev.* **2011,** *12*, 209. doi: 10.1016/j.jphotochemrev.2011.09.001

(39) Poonia, N. S.; Bajaj, A. V. *Chem. Rev.* **1979,** *79*, 389. doi: 10.1021/cr60321a002

(40) Abdullah, A.; Roxburgh, C. J.; Sammes, P. G. *Dyes and Pigments* **2008,** *76*, 319. doi: 10.1016/j.dyepig.2006.09.002

(41) Ipe, B. I.; Mahima, S.; Thomas, K. G. *J. Am. Chem. Soc.* **2003,** *125*, 7174. doi: 10.1021/ja0341182

(42) Nolan, E. M.; Lippard, S. J. *Accounts Chem. Res.* **2008,** *42*, 193.

(43) Huang, S.; Clark, R. J.; Zhu, L. *Org. Lett.* **2007,** *9*, 4999. doi: 10.1021/ol702208y

(44) Kowalczyk, T.; Lin, Z.; Voorhis, T. V. *J. Phys. Chem. A* **2010,** *114*, 10427.

(45) Winkler, J. D.; Bowen, C. M.; Michelet, V. *J. Am. Chem. Soc.* **1998,** *120*, 3237. doi: 10.1021/ja974181p

(46) Zhao, J.; Nelson, D. J. *J. Inorg. Biochem.* **2005,** *99*, 383. doi: 10.1016/j.jinorgbio.2004.10.005

(47) Torrado, A.; Walkup, G. K.; Imperiali, B. *J. Am. Chem. Soc.* **1998,** *120*, 609. doi: 10.1021/ja973357k

(48) Saghatelian, A.; Völcker, N. H.; Guckian, K. M.; Lin, V. S. Y.; Ghadiri, M. R. *J. Am. Chem. Soc.* **2002,** *125*, 346.

(49) Qu, D. H.; Ji, F. Y.; Wang, Q. C.; Tian, H. *Adv. Mater.* **2006,** *18*, 2035. doi: 10.1002/adma.200600235

(50) de Sousa, M.; Kluciar, M.; Abad, S.; Miranda, M. A.; de Castro, B.; Pischel, U. *Photochem. Photobiol. Sci.* **2004,** *3*, 639. doi: 10.1039/b406415a